Electronic Supplementary Material (ESI) for ChemComm.
This journal is © The Royal Society of Chemistry 2015

Supplementary Information

Stable and efficient hole transporting materials with dimethylfluorenylamino moiety for perovskite solar cells

Hyeju Choi,[a] Jin Woo Cho,[b] Moon-Sung Kang,[c] Jaejung Ko [*,a]

[a] *Department of Advanced Material Chemistry, Korea University Sejong Campus, Sejong-ro 2511, Sejong City, 339-700, Korea. Fax: +82-41-867-1331; Tel: +82-41-860-1337; E-mail: jko@korea.ac.kr*

[b] *Advanced Analysis Center, Korea Institute of Science and Technology(KIST), Hwarang-ro 14-gil 5, Seongbuk-gu, Seoul, 136-791, Republic of Korea.*

[c] *Department of Environmental Engineering, Sangmyung University, 300 Anseo-dong, Dongnam-gu, Cheonan-si, Chungnam 330-720, Republic of Korea*

Contents

Materials and HTM synthesis

Most reactions were performed under a nitrogen atmosphere. All reagents were purchased from commercial suppliers such as Sigma-Aldrich, Alfa, and TCI. 2,6,10-Tribromo-4,4,8,8,12,12-hexamethyl-4*H*,8*H*,12*H*benzo[1,9]quinolizino[3,4,5,6,7]acridine **(1)**,[1] tris(4-bromophenyl)amine **(2)**,[1] and *N*-(9,9-Dimethyl-9*H*-fluoren-2-yl)-9,9-dimethyl-*N*-(4-(4,4,5,5-tetramethyl-1,3,2-dioxaborolan-2-yl)phenyl)-9*H*-fluoren-2-amine **(3)**[2] were synthesized using a procedure of previous literature.

^{1}H and ^{13}C NMR spectra were recorded on a Varian Mercury 300 spectrometer. Chemical shifts δ were calibrated against TMS as an internal standard. Elemental analyses were performed with a Carlo Elba Instruments CHNS-O EA 1108 analyzer. The absorption and photoluminescence spectrometer were recorded on a Perkin-Elmer Lambda 2S UV-visible spectrometer and a Perkin LS fluorescence, respectively.

Cyclic voltammetry was carried out with a BAS 100B (Bioanalytical Systems, Inc.). Redox potential of materials was measured in dichloromethane solution with 0.1 M (n-$C_4H_9)_4NPF_6$ as the supporting salt. The platinum working electrode consisted of a platinum wire sealed in a soft glass tube with a surface of 0.785 mm^2, which was polished down to 0.5 μm with Buehler polishing paste prior to use in order to obtain reproducible surfaces. The counter electrode consisted of a platinum wire and the reference electrode was an Ag/AgCl secondary electrode.

Tris[[*N*-(9,9-dimethyl-9*H*-fluoren-2-yl)-9,9-dimethyl-*N*-phenyl-9*H*-fluoren-2-amine]-2,6,10-yl]-4,4,8,8,12,12-hexamethyl-4*H*,8*H*,12*H*-benzo[1,9]quinolizino[3,4,5,6,7]acridine (DMFA-FA). A mixture of compound 1 (0.21 g, 0.35 mmol), compound 3 (0.94 g, 1.56 mmol), and $Pd(PPh_3)_4$ (0.04 g, 0.04 mmol), aqueous potassium carbonate solution (0.72 g in 15 mL H_2O) in tetrahydrofuran (50 mL) was refluxed for 2 days. Subsequently, the mixture was cooled down to room temperature. Waster was added and the resulting solution was extracted three times with diethyl ether (50 mL). The combined organic layers were washed with brine, dried ($MgSO_4$). The solvent was removed *in vacuo* and the residue was purified by column chromatography on silicagel eluting with CH_2Cl_2/Hexane (1:4) to give DMFA-FA. ^{1}H NMR (300 MHz, CD_2Cl_2): δ 7.70-7.62 (m, 24H), 7.42 (d, 6H, J=7.2 Hz), 7.33-7.27 (m, 24H), 7.14 (d, 6H, J=8.4 Hz), 1.80 (s, 18H), 1.44 (s, 36H). ^{13}C NMR (75 MHz, $CDCl_3$): δ 155.1, 153.6, 147.4, 146.9, 139.0, 135.1, 134.9, 134.1, 130.4, 126.5, 124.9, 124.0, 123.3, 122.5, 122.0, 121.7, 121.2, 119.9, 118.7, 117.9, 46.9, 35.9, 33.4, 26.7, 26.5. MS: *m/z* 1791.91 [M^+]. Anal. Calcd. for $C_{135}H_{114}N_4$: C, 90.46; H, 6.41.

Tris[[*N*-(9,9-dimethyl-9*H*-fluoren-2-yl)-9,9-dimethyl-*N*-phenyl-9*H*-fluoren-2-amine]-*p*-phenylene]amine (DMFA-TPA). The product DMFA-TPA was prepared using the same procedure for DMFA-FA except that compound 2 (0.20 g, 0.41 mmol) were used instead of compound 1. ^{1}H NMR (300 MHz, CD_2Cl_2): δ 7.67-7.53 (m, 24H), 7.27 (d, 6H, J=6.9 Hz), 7.34-7.21 (m, 30H), 7.11 (d, 6H, J=8.1 Hz), 1.41 (s, 36H). ^{13}C NMR (75 MHz, $CDCl_3$): δ 155.6, 154.1, 147.8, 147.4, 139.4, 135.0, 134.5, 127.7, 127.4, 126.9, 124.6, 123.5, 122.9, 121.0, 119.7, 119.0, 110.4, 47.2, 27.2. MS: *m/z* 1671.81 [M^+]. Anal. Calcd. for $C_{126}H_{102}N_4$: C, 90.50; H, 6.15.

Reference

[1] H. Choi, S. Paek, N. Lim, Y. H. Lee, M. K. Nazeeruddin, J. Ko, *Chem. Eur. J*. 2014, **20**, 10894.

[2] J.-J. Kim, H. Choi, J.-W. Lee, M.-S. Kang, K. Song, S. O. Kang, J. Ko, *J. Mater. Chem*., 2008, **18**, 5223.

Solar cell fabrication

F-doped tin oxide (FTO) glass plates (Pilkington, TEC-8) were cleaned in a detergent solution using an ultrasonic bath for 30 min, rinsed with water and ethanol. The compact TiO_2 layer was deposited on the etched FTO substrate by spray pyrolysis at 450 ^oC, using titanium diisopropoxide bis(acetylacetonate) solution.

The FTO glass plates were immersed in 40 mM $TiCl_4$ aqueous solution at 70 ^oC for 30 min and then sintered at 500 ^oC for 30 min. Mesoporous TiO_2 films was deposited by spin coating of a diluted TiO_2 paste (Dyesol 18NR-T, 1:3.5 w/w diluted with ethanol) at 5000 rpm for 30 s. The films were successively sintered at 500 ^oC. The PbI_2 in DMF solution (1.0 M) was dropped on the TiO_2/FTO substrate and then spin-coated at 6500 rpm for 30 s and dried on a hot plate at 70 ^oC for 30 min. After cooling down, the film was dipped into a CH_3NH_3I/2-propanol solution (8 mg/mL) for 25 s, and dried at 70 ^oC for 15 min. For a deposition of HTM layers, DMFA-FA/chlorobenzene (20 mM) and DMFA-TPA/chlorobenzene (25 mM) solutions were prepared with two additives. 3.5 μL lithium bis(trifluoromethanesulonyl)imide (Li-TFSI)/acetonitrile (520 mg/1 mL) and 8.0 μL (4-*tert*-butylpyridine) (TBP) were added to the HTM/chlorobenzene solutions as additives. The HTMs were spin-cast on top of the $CH_3NH_3PbI_3/TiO_2$/FTO substrate at 3000 rpm. Finally, the device was pumped down to lower than 10^{-5} torr and a ~60 nm thick Au counter electrode was deposited on top.

Solar cell performance measurement

Solar cell efficiencies were evaluated under simulated one sun irradiation from a Xe arc lamp with an AM 1.5 global filter. Irradiance was characterized using a calibrated spectrometer and illumination intensity was set using an NREL certified silicon diode with an integrated KG1 optical filter: spectral mismatch factors were calculated for each device in this report to be less than 5%. Short circuit currents were also found to be with 5% of values calculated using the integrated external quantum efficiency (EQE) spectra and the solar spectrum. The EQE was measured by underfilling the device area using a reflective microscope objective to focus the light output from a 75 watt Xe lamp, monochromator, and optical chopper; photocurrent was measured using a lock-in amplifier and the absolute photon flux was determined by a calibrated silicon photodiode. The LHE spectrum of HTMs was measured from the perovskite and HTM extinction coefficient and the optical path length within the film.[3] The LHE spectrum evaluated using Lambert-Beer law.

Reference

[3] Y. Tachibana, K. Hara, K. Sayama, H. Arakawa, *Chem. Mater*. 2002, **14**, 2527.

Figure S1 Schematic diagram for the synthesis of the **DMFA-FA** and **DMFA-TPA**.

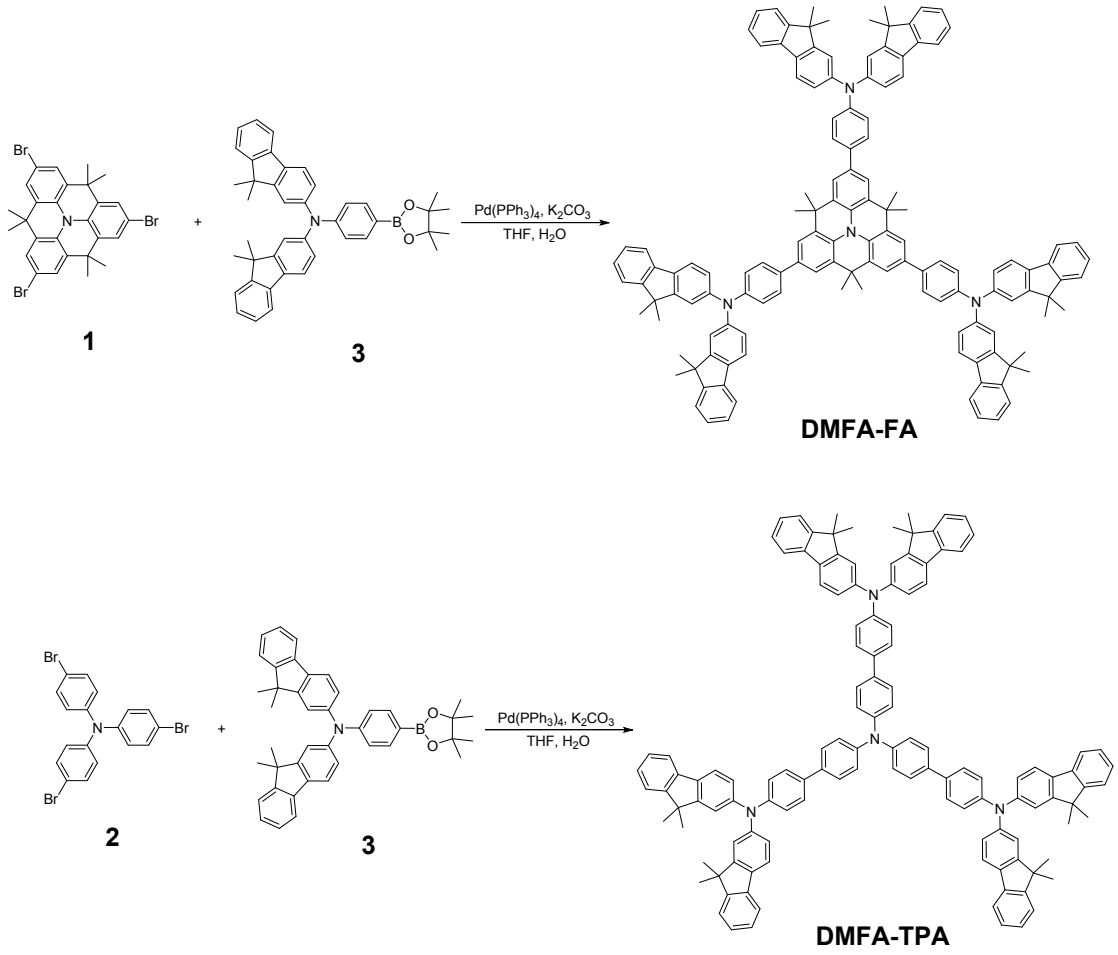

Table S1 Optical and redox parameters of the compounds

HTM	λ_{abs}[a]/nm (ε/$M^{-1}cm^{-1}$)	λ_{PL}[a]/nm	HOMO (eV)[b]	LUMO (eV)[c]	E_{gap} (eV)[d]
DMFA-FA	377 (191 500)	434	-5.21	-2.23	2.98
DMFA-TPA	371 (332 700)	430	-5.25	-2.26	2.99

[a] UV-vis absorption spectra and fluorescence spectra were measured in chlorobenzene solution. [b] Redox potential of the compounds were measured in CH_2Cl_2 with 0.1 M $(n\text{-}C_4H_9)_4NPF_6$ with a scan rate of 100 mVs^{-1} (*vs*. Fc/Fc^+). [c] $E_{LUMO} = E_{HOMO} + E_{gap}$ [d] E_{gap} was calculated from the absorption thresholds from absorption spectra.

Figure S2 Electrochemical characterization of the **DMFA-FA** and **DMFA-TPA** in dichloromethane/(n-$C_4H_9)_4NPF_6$ (0.1 M), scan speed 100 mV/s, potentials *vs*. Ag/Ag^+.

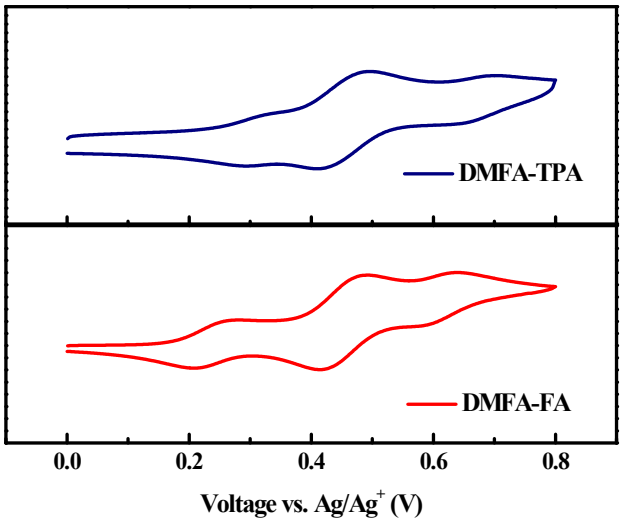

Figure S3 (a) LHE spectra of **DMFA-FA** (red line) and **DMFA-TPA** (blue line), (b) APCE spectra derived from the IPCE and LHE.

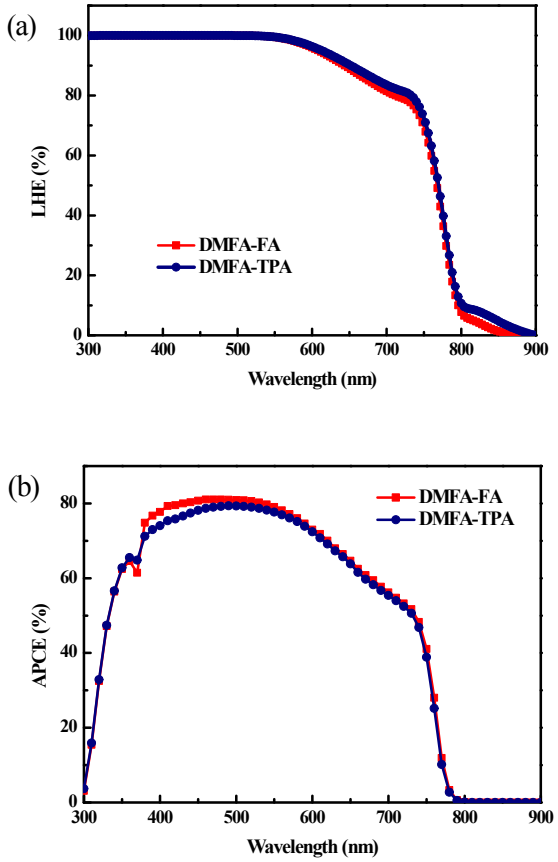

Figure S4 Space charge limitation of current in the *J-V* characteristics of the solar cells with different HTMs.

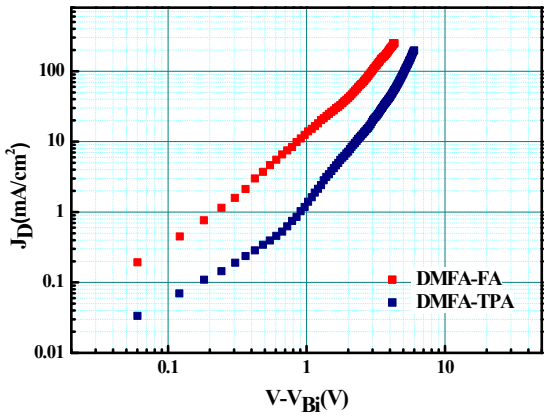

Figure S5 Histogram of the solar cell efficiencies obtained from the (a) **DMFA-FA**, (b) **DMFA-TPA**, and (c) **spiro-OMeTAD** based hybrid solar cells.

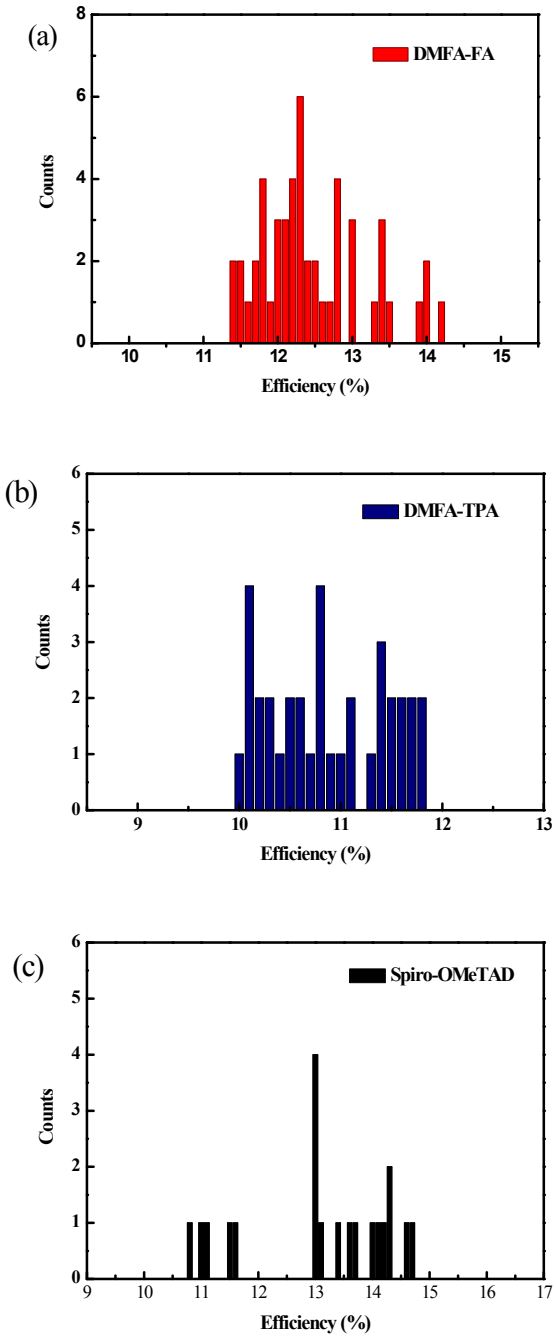

Figure S5 Thermo-gravimetric analysis of (a) **DMFA-FA** and (b) **DMFA-TPA**.

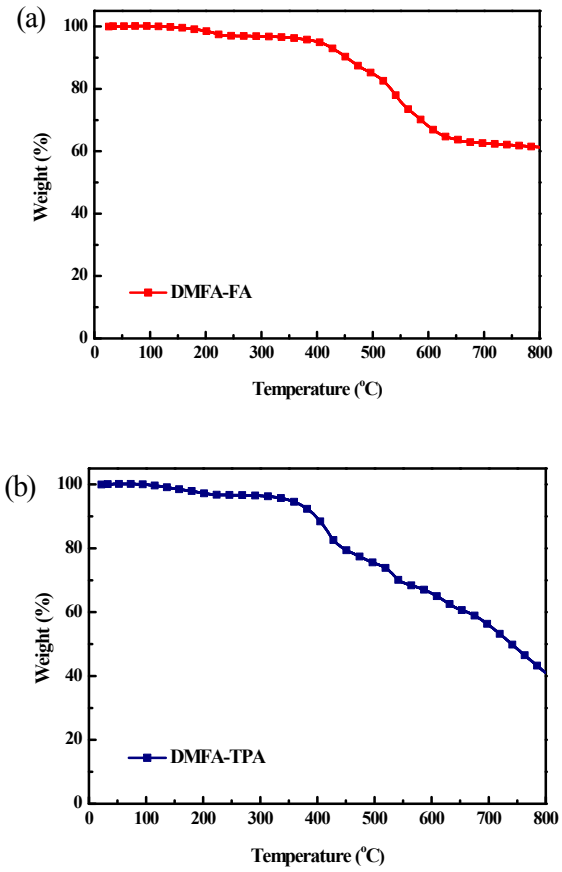

Figure S6 *J-V* characteristics of the solar cells with (a) **DMFA-FA** (■), (b) **DMFA-TPA** (●), and (c) **spiro-OMeTAD** (▲) as the HTMs, respectively, evaluated under one sun condition with different scan directions.

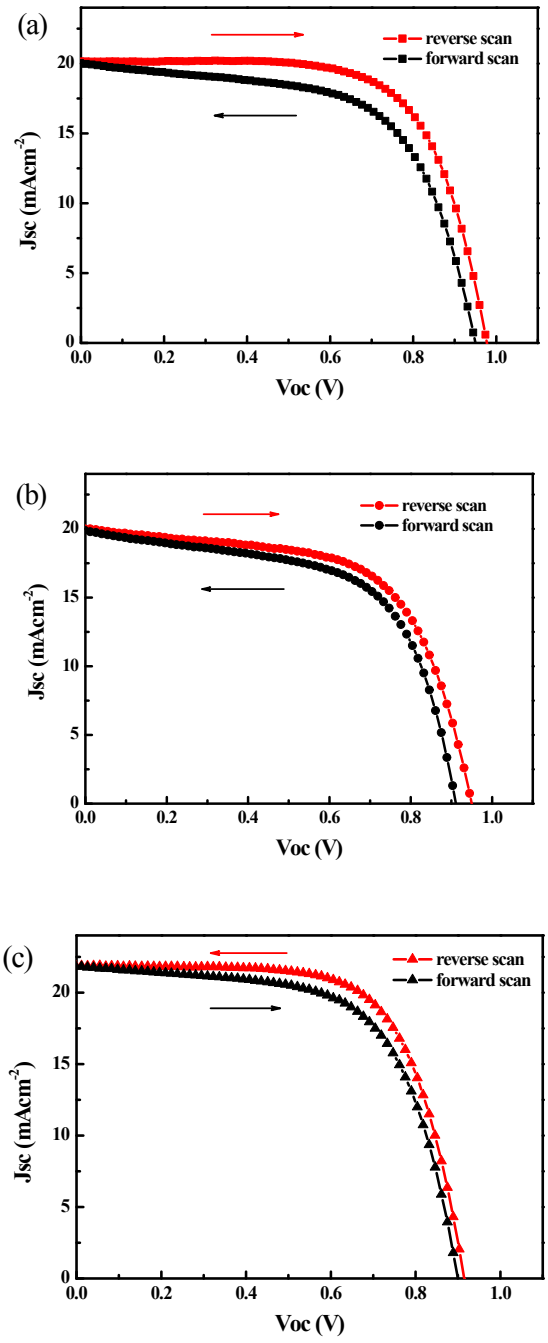

Table S2 Summary of photovoltaic performances of the solar cells with (a) **DMFA-FA** (■), (b) **DMFA-TPA** (●), and (c) **spiro-OMeTAD** (▲) as the HTMs, respectively, evaluated under one sun condition with different scan directions

HTM		J_{sc} (mAcm^{-2})	V_{oc} (V)	FF	η (%)
DMFA-FA	Reverse	20.147	0.9776	0.679	13.37
	Forward	20.017	0.9501	0.614	11.67
	Average	20.082	0.9639	0647	12.52
DMFA-TPA	Reverse	20.017	0.9501	0.614	11.67
	Forward	19.879	0.9111	0.601	10.88
	Average	19.948	0.9306	0.608	11.28
Spiro-OMeTAD	Reverse	21.873	0.9148	0.674	13.48
	Forward	21.843	0.8997	0.631	12.41
	Average	21.858	0.9073	0.653	12.95

Performances of devices were measured with 0.16 cm^2 working area.